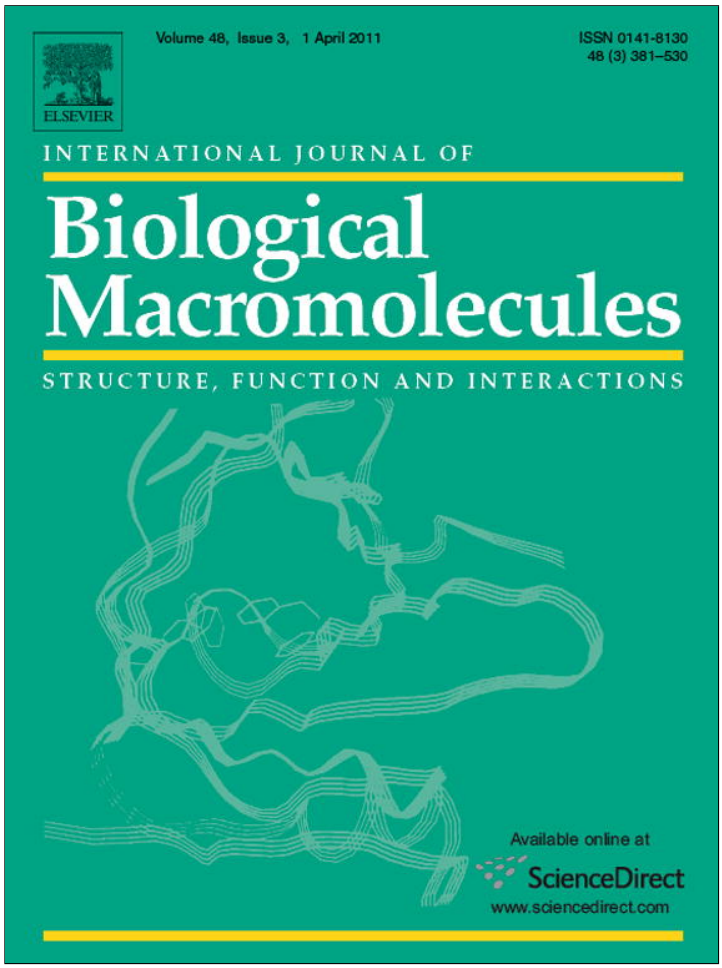

International Journal of Biological Macromolecules 48 (2011) 459–465

Contents lists available at ScienceDirect

International Journal of Biological Macromolecules

journal homepage: www.elsevier.com/locate/ijbiomac

The 1.6 Å resolution structure of activated D138L mutant of catabolite gene activator protein with two cAMP bound in each monomer

Wenbing Tao[a,1], Zengqiang Gao[b,1], Zhengya Gao[a], Jiahai Zhou[c], Zhongxian Huang[a], Yuhui Dong[b,*], Shaoning Yu[a,**]

[a] Department of Chemistry and Institutes of Biomedical Science, Fudan University, Shanghai 200433, China
[b] Institute of High Energy Physics, Chinese Academy of Sciences, Beijing 100049, China
[c] Institute of Organic Chemistry, Chinese Academy of Sciences, Shanghai 200032, China

ARTICLE INFO

Article history:
Received 31 August 2010
Received in revised form
27 December 2010
Accepted 10 January 2011
Available online 19 January 2011

Keywords:
Catabolite gene activator protein (CAP)
Cyclic AMP (cAMP)
Transcription
Allostery
X-ray crystallography

ABSTRACT

The X-ray crystal structure of the cAMP-liganded D138L mutant of *Escherichia coli* catabolite gene activator protein (CAP) was determined at a resolution of 1.66 Å. This high resolution crystal structure reveals four cAMP binding sites in the homodimer. Two anti conformations of cAMPs (*anti*-cAMP) locate between the β-barrel and the C-helix of each subunit; two syn conformations of cAMPs (*syn*-cAMP) bind on the surface of the C-terminal domain. With two *syn*-cAMP molecules bound, the D138L CAP is highly symmetrical with both subunits assuming a "closed" conformation. These differences make the hinge region of the mutant more flexible. Protease susceptibility measurements indicate that D138L is more susceptible to proteases than that of wild type (WT) CAP. The results of protein dynamic experiments (H/D exchange measurements) indicate that the structure of D138L mutant is more dynamic than that of WT CAP, which may impact the recognition of specific DNA sequences.

1. Introduction

The expressions of at least 150 genes involved in various cellular functions in *Escherichia coli* are regulated by catabolite gene activator protein (CAP, also referred as cAMP receptor protein) [1–3]. It has been reported that CAP undergoes allosteric conformational changes upon binding of cAMP that enable the protein to recognize specific DNA sequences, and interact with RNA polymerase (RNAP) [4–7]. As a transcription factor, CAP has been studied extensively by molecular dynamics [8,9], biochemical [6,10,11], and biophysical techniques [12,13], in order to understand the allosteric mechanism induced by cAMP binding. It has a broad significance for a precisely determined structure of both cAMP free CAP [1] and CAP–cAMP complex [2], since CAP has become a model for both cAMP-binding and DNA-binding motifs found in many other proteins, such as protein kinase A [14,15], exchange protein activated by cAMP [16,17], and cyclic nucleotide-gated ion channels [18,19], although each protein involves in unique process of structural activation.

The three-dimensional crystal structure of CAP–cAMP complex was first determined in 1981 [20], and was subsequently refined to 2.1 Å in 2000 [2]. The structure of CAP–cAMP–DNA complex was determined in 1991 [7] and the structure of CAP–cAMP–DNA–RNAP complex was determined in 2002 [21]. All structures showed that CAP from *E. coli* is a dimeric protein composed of two chemical identical subunits with 209 amino acid residues. Each subunit contains two domains: a larger N-terminal domain containing the cAMP binding site and a smaller C-terminal domain capable of binding to DNA through a helix-turn-helix motif. The structure of wild type (WT) CAP–cAMP complex revealed that one subunit is in a "closed" form, where the C-terminal domain swung in toward the α-helical interface, and the other subunit is in an "open" form, where the C-terminal domain swung away from the α-helical interface [22]. The two functional domains are connected by a hinge region, typically defined as the L134–D138 region, which accommodates the movement of the small domain from "open" to "closed" conformation. The structure of T127L/S128A double mutant has revealed a third cAMP binding site which is located in the "closed" subunit [23]. However, the structure of CAP–DNA complex showed that there are two cAMP molecules bound to each CAP monomer in the presence of DNA, and each monomer has a "closed" conformation [5].

* Corresponding author. Tel.: +86 10 88233090; fax: +86 10 88233201.
** Corresponding author. Tel.: +86 21 55664974; fax: +86 21 65641740.
E-mail addresses: dongyh@ihep.ac.cn (Y. Dong), yushaoning@fudan.edu.cn (S. Yu).
[1] These authors equally contributed to this work.

0141-8130/$ – see front matter © 2011 Elsevier B.V. All rights reserved.
doi:10.1016/j.ijbiomac.2011.01.009

It is difficult to speculate on the nature of conformational changes that take place upon cAMP binding, until the structures of the unliganded D138L mutant and *apo*-WT CAP were determined recently [24], although the resolution of *apo*-WT CAP is only 3.6 Å (PDB code 3HIF). The structure of *apo*-D138L CAP mutant has been solved to a resolution of 2.2 Å (PDB code 3FWE) [24], which is the only high resolution unliganded *E. coli* CAP structure currently available. The structure of *apo*-WT CAP reveals that the DNA recognition helices (F-helices) are buried into the core structure and the two DNA binding domains are dimerized into one rigid body. The latter explains the low DNA binding affinity in the absence of cAMP. The structural comparison of the liganded and unliganded WT-CAP suggests that cAMP binding to CAP induces a large conformational change and cAMP itself stabilizes the active conformation through its interactions with the C-helices [24].

The D138L mutant showed a reduced affinity for DNA, however, it exhibited a subunit association similar to that of WT CAP, and furthermore it stabilized the inactive form of the protein. In this work, the X-ray crystal structure of D138L–cAMP complex has been determined to a resolution of 1.66 Å, which is the highest resolution structure of CAP, containing four cAMP molecules. Hydrogen–deuterium (H–D) exchange by FT-IR and proteolytic digestion were employed to investigate protein dynamics. The relationship between protein structure, protein dynamics, and DNA binding affinity is discussed.

2. Materials and methods

2.1. Materials

The glycerol, kanamycin disulfate salts, HEPES, isopropylthio galactopyranoside (IPTG), phenylmethylsulfonyl fluoride (PMSF), Tris–HCl, dithiothreitol (DTT), and sodium salt of cAMP were all reagent grade from Sigma. Bio-Rex70 was purchased from Bio-Rad Laboratories, Inc., and the hydroxyapatite, 4K polyethylene glycol was obtained from Fluka, Phenyl Sepharose was purchased GE Healthcare.

2.2. Methods

2.2.1. Site-directed mutagenesis

The Promega Altered Site in vitro Mutagenesis System was used to introduce specific point mutations into the crp gene using a previously published procedure [11,25]. The desired mutants were directly screened by DNA sequencing.

2.2.2. Expression and purification

The D138L CAP mutant was overexpressed in BL21 cells. The cells were induced with 1 mM IPTG after growth to OD_{600} ~0.5–0.8 in Luria Broth supplemented by kanamycin at 37 °C, and harvested approximately 5 h after induction.

Approximately 50 g cells were resuspended with 60 mL Buffer A (50 mM Tris–HCl pH 7.8, 1 mM EDTA, 100 mM KCl, 1 mM DTT, 0.2 mM PMSF, 5% Glycerol), homogenized at 4 °C, and then lysed by French Press. The lysate was clarified by centrifugation and followed by the addition of ~35 g BioRex70 that had been preequilibrated at pH 7.5 with buffer A, then gently mixed for 30 min. The supernatant was removed and replaced with a 200 mL fresh Buffer A. After gently stirring, the supernatant was removed again. This procedure was repeated approximately 5 times until $OD_{278}/OD_{260} > 1.5$.

The matrix was slowly packed into a column, washed with ~100 mL Buffer A. The D138L CAP mutant was gradient-eluted with 120 mL Buffer A-120 mL 1.0 M KCl. After elution the OD of each tube was examined and protein was pooled. The protein solution was dialyzed overnight against Buffer A.

The protein sample was then centrifuged to remove any precipitate, loaded on a column which was packed with approximately 15 g hydroxyapatite, and washed with ~50 mL Buffer B (50 mM K_2HPO_4–KH_2PO_4, pH 7.5, 1 mM EDTA, 1 mM DTT, 10% Glycerol). The D138L CAP was gradient-eluted with 120 mL Buffer B-120 mL 0.50 M K_2HPO_4–KH_2PO_4, pH 7.5. The protein samples were pooled according to gel. Solid $(NH_4)_2SO_4$ was added to a final concentration of 1.2 M. The sample was then loaded onto a Phenyl Sepharose column that was pre-washed with ~1 L ddH_2O and equilibrated with ~300 mL Buffer C (1.2 M $(NH_4)_2SO_4$, 50 mM Tris–HCl, pH 7.8, 100 mM KCl, 1 mM EDTA, 1 mM DTT). After sample loading, the column was washed with ~50 mL of Buffer C and the protein was gradient-eluted with 100 mL Buffer C-100 mL ddH_2O and pooled. A 20% glycerol was added to the sample and kept at −20 °C. The concentration of D138L-CAP was determined by UV–Vis spectroscopy using an extinction coefficient of 40,800 M^{-1} cm^{-1} at 278 nm [8].

2.2.3. Crystallization and data collection

Crystallization was carried out using the hanging-drop method. The initial screening was performed using Hampton Research Crystal Screen kit I, II and Index (Hampton Research, Riverside, CA, USA) at 293 K. Each drop contains 2 μL proteins and 2 μL reservoir solutions and equilibrated against 500 μL reservoir solution in the well. Crystals appear under the condition of 10% PEG4000, 7% isopropanol, 3 mM cAMP and 0.1 M HEPES pH 6.1 after 1 day. The crystal belongs to the space group P21 with unit cell parameters $a = 45.5$, $b = 102.2$, $c = 53.9$ Å, $\beta = 110.9°$.

The crystal was transferred into the cryo-protectant solution (reservoir solution containing 20% glycerol) before being flash-frozen at 100 K. The X-ray diffraction data were collected on beamline BL-17A at the Tsukuba Photon Factory (Ibaraki, Japan) with an ADSC Quantum 270 detector. All the data were processed with HKL2000 [25].

2.2.4. Structure determination and refinement

The initial phases for the structure of D138L–cAMP was solved by Molecular Replacement using Crystallography and NMR System (CNS) program with the monomer structure of the cAMP-liganded T127L/S128A double mutant CAP (PDB code 1HW5-A) as a search model. The structure was solved following the flowchart provided in CNS. Firstly, the molecular orientation and position in the unit cell were obtained by the cross rotation and translation functions, respectively. Secondly, another translation search was performed in order to complete the dimer. Finally, rigid body refinement was performed. The initial structure was refined following the flowchart provided in CNS. After annealing and energy minimizing using anneal and minimize programs, the structure was refined by the Phenix program [26]. Some biases were corrected manually using the program COOT [27]. After several cycles of refinement the structure was refined to a final resolution of 1.66 Å with an R-factor of 20.4% and free R-factor of 24.1%. The program Procheck from CCP4 [28] was used to assess the stereochemical quality of the final refined model.

2.2.5. Protease digestion

Subtilisin and chymotrypsin were employed for the proteolytic digestions, which were carried out in a reaction volume of 50 μL containing 15 μM CAP and 8 μg/mL protease at room temperature in TEK100 buffer (50 mM Tris, 1 mM EDTA, 100 mM KCl at pH 7.8). The reaction started by addition of 2 μL (200 μg/mL) protease, and stopped by addition of 1 μL 100 mM PMSF in 2-propanol to a final concentration of 1 mM. The reaction time is 80 min for subtilisin and 120 min for chymotrypsin. 15 μL aliquots of the reaction mixture were withdrawn and loaded onto a 15% SDS-PAGE slab gel for electrophoresis analysis. Gels were stained with Coomassie blue.

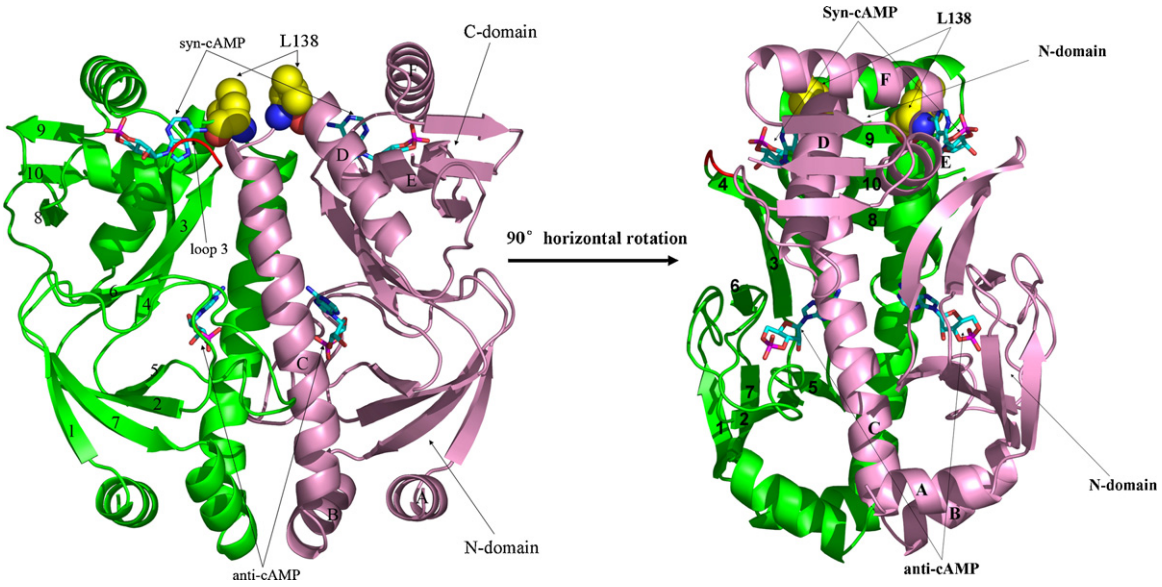

Fig. 1. Structure of the liganded CAP mutant D138L. The α-helices are labeled A to F and β-strands are numbered 1–10. Subunit A is colored in green and subunit B in pink. (For interpretation of the references to color in this figure legend, the reader is referred to the web version of the article.)

2.2.6. H/D exchange monitored by FT-IR spectroscopy

FT-IR spectra were measured with a Bomem MB series Fourier Transform Infrared Spectrometer (Quebec, Canada) equipped with a dTGS detector and purged constantly with dry air. Each 100 μL of (~100 μM) protein solution in TEK100 buffer was lyophilized. Samples for the exchange experiment were prepared by dissolving each 100 μL of lyophilized protein or buffer in 100 μL D_2O. The reconstituted sample was injected into an IR cell with CaF_2 windows and a 50 μm spacer. The spectra were recorded with a kinetic scanning mode at 1, 2, 3, 4, 5, 6, 7, 8, 9, 10, 11, 15, 20, 30, 40, 50, 60, 90, 120, 150, and 180 min after the addition of D_2O. Eight scans were collected for each time interval from 1 to 10 min; 64 and 128 scans for each time interval from 11 to 90 min and longer, respectively. Reference spectra were recorded under identical conditions with only the corresponding buffer in the cell. Protein spectra were subtracted using a previously established protocol [8]. A straight base line between 2000 and 1750 cm^{-1} was used as the standard for judging the successfulness of buffer subtraction [29]. To compare the FT-IR spectra in H_2O and D_2O, we normalized the amide I band in H_2O to the amide I band in D_2O at 1 min. The spectrum collected after 24 h exchange was used as the fully deuterated protein reference.

The H–D exchange of protein was monitored by observing the apparent intensity changes of the amide II band, located around 1550 cm^{-1}, which is attributed to a combination of N–H in-plane bending and C–N stretching vibrations in the peptide bond, because this band does not adversely interfere with the absorption bands of H_2O, HOD, or D_2O. As the N–H in protein is exchanged to N–D in D_2O, the absorption peak of N–D bending vibration at about 1450 cm^{-1} is strengthened, while the N–H absorption peak decreases. The fraction of the unexchanged amide proton, F, was calculated at various time intervals using Eq. (1):

$$F = \frac{A_{II} - A_{II\infty}}{A_I \omega} \quad (1)$$

where A_I and A_{II} are the absorbance maximum of the amide I and II bands, respectively. $A_{II\infty}$ is the amide II absorbance maximum of fully deuterated protein; and ω is the ratio of A_{IIo}/A_{Io}, with A_{IIo} and A_{Io} being the respective absorbance maximum for the amide II and amide I bands of protein in H_2O [29,30].

The exchange kinetic parameters were fitted from the equation below:

$$F = A_1 e^{-k_1 t} + A_2 e^{-k_2 t} + C \quad (2)$$

where F is amide proton fraction at given time t; k_1 and k_2 are the intermediate and slow exchange rate, respectively; A_1, A_2 and C are the constants; F_0 is the remaining amide proton fraction at 1 min.

2.3. Accession numbers

Coordinates and structure factors have been deposited in the Protein Data Bank with accession number 3KCC.

3. Results

3.1. Three dimensional structure of D138L CAP

The X-ray crystallographic data collection statistics are shown in Table 1, and the overall structures are shown in Fig. 1. Both subunits in D138L CAP are in the "closed" conformation. 10 residues in subunit A (V1–T7 and G207–R209) and 11 residues in subunit B (V1–D8 and G207–R209) are missing because of poor electron density. Each subunit has two domains: the larger N-terminal cAMP binding domain and the smaller C-terminal DNA-binding domain. The two domains are connected via a hinge consisting of residues F136–T140. The residues between L151 and M164 in the subunit A have weak electron densities, whereas the same region in the subunit B is more interpretable. Four cAMP molecules are shown to associate with the two subunits in the asymmetric unit: two are *anti*-cAMP, located between the β-barrel and the C-helix of each subunit, and the other two are *syn*-cAMP, binding to the surface of C-terminal domain.

Although both subunits are in the "closed" conformation, the relative orientation between the two domains in each subunit is somewhat different. The DNA binding domain is closer to the cAMP-binding domain in subunit B than in subunit A. Accounting for most of the RMSD difference of 0.96 Å between the two subunits, the RMSD differences between the two cAMP binding domains and the two DNA binding domains, however, are only 0.29 and 0.32 Å, respectively (Fig. 2).

Table 1
Data collection statistics. Values in parentheses are for the highest resolution shell.

Data collection	
Space group	$P2_1$
Unit cell (Å)	a = 45.5, b = 102.2, c = 53.9, β = 110.9
Solvent content (%)	38.9
Resolution range (Å)	50–1.6 (1.66–1.6)
R_{sym} (%)	5.8 (48.3)
Completeness (%)	98.7 (96.4)
Redundancy	7.3 (5.9)
I/σ	28.0 (3.5)
Refinement	
R_{work} (R_{free}) (%)	20.4 (24.1)
No. of residues	397
Protein atoms (water)	3087 (298)
Ligand (numbers)	CMP (4)
RMSD bond lengths (Å)	0.006
RMSD bond angles (°)	1.2
<B factor> protein (Å^2)	27.4
<B factor> ligand (Å^2)	21.9
<B factor> solvent (Å^2)	36.9
Ramachandran	
Core (%)	95.2
Allowed (%)	4.8
Generously allowed (%)	0.0
Disallowed (%)	0.0

3.2. Cyclic AMP binding sites

The *anti*-cAMP binding sites in D138L CAP are nearly identical to those in the structures of CAP–cAMP (PDB code 1G6N) and CAP–DNA (PDB code 2CGP). The *syn*-cAMP binding sites are composed of K57, E58, G173, Q174, and G177 to E181 from the same subunit and A135 from the other subunit (Fig. 3). The residues that interact with the *syn*-cAMP are similar to those in T127L/S128A CAP (PDB code 1HW5) and CAP–DNA complex (PDB code 2CGP). E58 and R180 interact directly with the *syn*-cAMP by the hydrogen bond between individual nitrogen atom(s) and oxygen atom(s) of phosphate group or ribose O2*. E181 interacts with *syn*-cAMP via a water molecule. It is noteworthy that A135 from subunit A interacts indirectly with N6 of *syn*-cAMP via a water molecule, whereas the same residue from subunit B interacts directly with N6. The left residues interact with *syn*-cAMP through hydrophobic contacts. As for the interaction type, the *syn*-cAMP binding sites in D138L CAP are similar to those in the CAP–DNA complex, because in T127L/S128A CAP two more residues (G56 and Q170) are included in the interaction of cAMP with protein. Meanwhile, Q174 and A177 both interact with cAMP via water molecules.

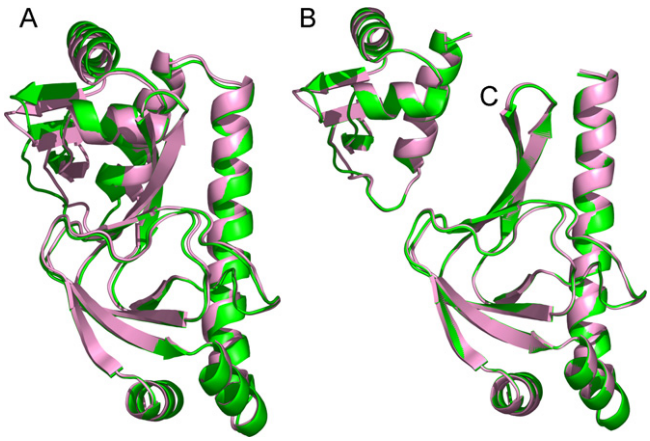

Fig. 2. Comparison of two subunits (A), two C-domains (B) and two N-domains (C) of D138L mutant. The RMSD between the two subunits is 0.96 Å, however, the RMSD differences between the two cAMP binding domains and the two DNA binding domains are only 0.29 and 0.32 Å, respectively.

3.3. Structural comparison of liganded D138L and WT CAP

The liganded WT CAP without DNA (PDB code 1G6N) shows an asymmetric homodimer, namely one subunit is in the "open" conformation, and the other in the "closed" conformation. There are two *anti*-cAMP molecules in WT CAP, whereas two additional *syn*-cAMP molecules are found in D138L CAP. Also the two subunits of D138L CAP are approximately symmetric.

Comparison of the closed subunit of WT CAP with D138L CAP reveals that the most significant difference appears in the β-flap which contains β3, β4 and loop 3 (Fig. 4). In D138L–cAMP complex, the loop is shortened by three residues and consists of only two residues E54–E55. In the meanwhile, β3 becomes two residues longer and spans residues S46–D53, and β4 becomes three residues longer spanning residues G56–N65. In addition, two shorter β-sheet strands, β2 and β9, are replaced by a loop in D138L–cAMP complex. Besides, the interaction between D138 oxygen atom and G141 nitrogen atom is hindered, and a water molecule is hydrogen bonded to the amide nitrogen atom of L138 residue.

3.4. Structural comparison of liganded and unliganded D138L CAP

Comparison of the structure of liganded D138L CAP to the previously determined structure of unliganded D138L CAP (PDB code 3FWE) reveals very little conformational alteration in the N-terminal cAMP-binding domains except the β-flap. On the other hand, the orientation of the DNA binding domains and the length of C and D helices differ dramatically between the two forms (Fig. 5). In the unliganded D138L, the D-helix extends 4 residues longer and spans residues 135–152, whereas in the D138L–cAMP complex only residues 139–152 form the D-helix. The length of the C-helix increases by 6 residues (G110–B130) or 1.5 helical turns from the unliganded to the liganded states, whereas the D-helix decreases by the same amount.

3.5. Sensitivity to proteolytic digestion

Limited proteolysis (for example use of subtilisin and chymotrypsin) can be employed to detect protein dynamics and conformational changes induced by binding of cAMP [4,6,31,32]. WT CAP is sensitive to proteases only in the presence of cyclic nucleotide. In the presence of cAMP, the subtilisin- and chymotrypsin-generated WT CAP cores were reported to terminate at residues 134 and 137, respectively, in the hinge region [1,4]. Both subtilisin and chymotrypsin were employed in this study to detect changes in the protein dynamics. The result shows that D138L mutant is sensitive to subtilisin and chymotrypsin in the presence of cAMP, and similar to WT, the proteolytic digestion pattern is biphasic as a function of cAMP concentration. An initial increase in the rate of proteolysis at low cAMP concentration (0–200 μM) is followed by a decrease in rate with further increase in cAMP concentration (0.5–50 mM) (Fig. 6). Furthermore, D138L is more sensitive to subtilisin and chymotrypsin than that of WT CAP in the presence of low concentration of cAMP (<200 μM), indicating a more dynamic structure at the hinge region (Fig. 6, gel-electrophoresis of subtilisin not shown). The results are consistent with the results of Ryu et al. [6].

3.6. H–D exchange rates of D138L and WT CAP

To explore and compare the protein dynamics of WT CAP and D138L mutant, H–D exchange rates of both WT and D138L were determined by FT-IR. While the spectra in H_2O exhibited amide I and II band maxima at 1652 and 1552 cm^{-1}, respectively, the spectra of the proteins in D_2O showed a time-dependent isotopic shift

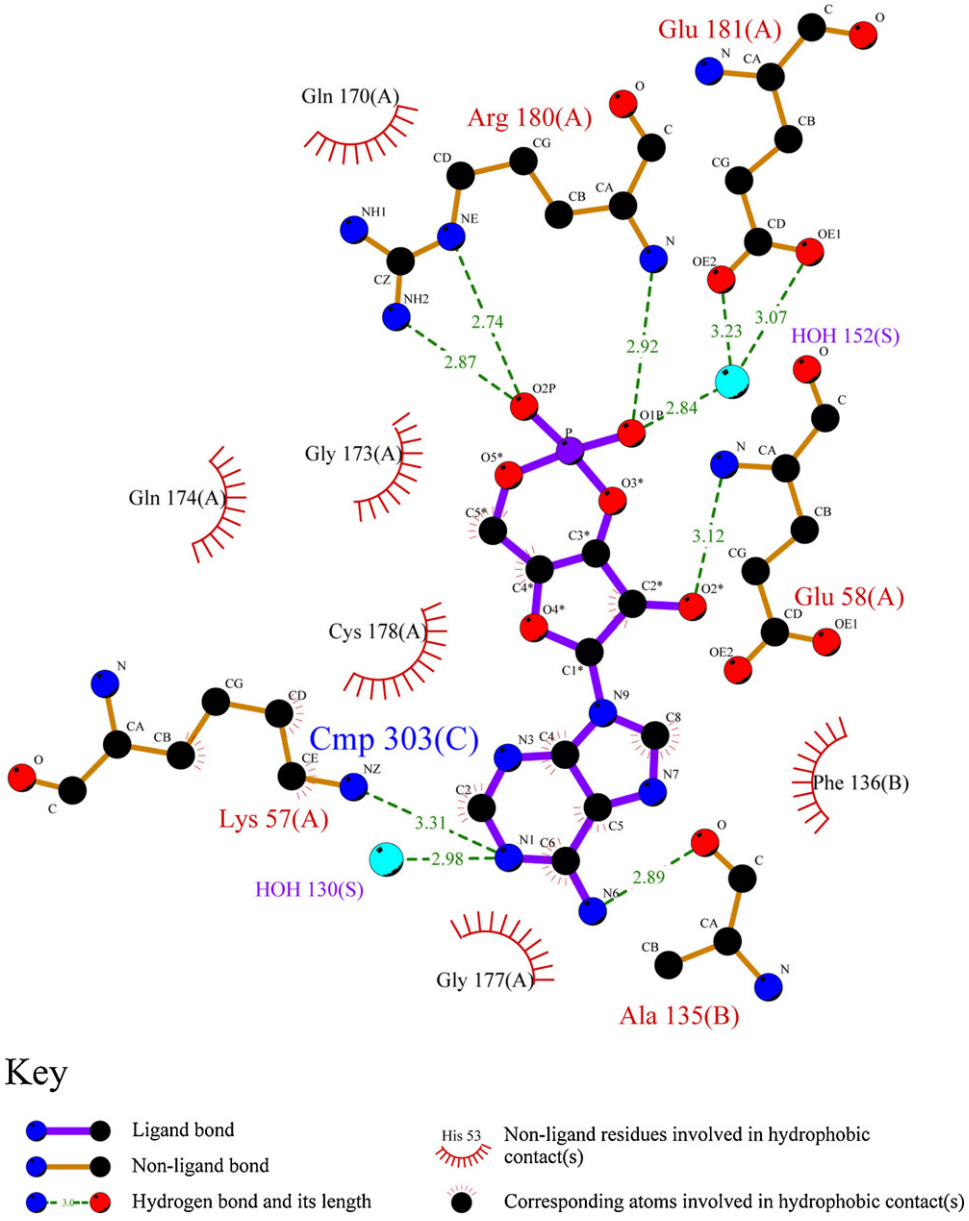

Fig. 3. Diagram of the *syn*-cAMP and the hydrogen-bond interactions that are made to it. The hydrogen-bond distances given are measured between the donor and the acceptor atoms in the structure. E181 makes a water-mediated interaction with the cAMP phosphate. A135 is from the other CAP subunit.

of the amide II band from 1548 to 1452 cm^{-1} (data not shown). This effect is indicative of NH to ND exchange of peptide backbone groups, which resulted in a downshift of approximately 100 cm^{-1} in the vibrational frequency of the amide II band [29]. Since the amide I band arises from the vibrational energy of C=O stretching, the effect of H–D exchange on the amide I second-derivative spectra is the consequence of an indirect effect on the changing of the strength of hydrogen bonding due to a H to D exchange.

The overall H–D exchange rates were estimated by plotting the fraction of unexchanged amide protons as a function of time (Fig. 7). Basically, all amide protons in proteins can be divided into three categories [33,34]: (1) the fast exchange protons located most likely on the surface of proteins or in regions that are easily solvent accessible; (2) amide protons with intermediate exchange rates, located in flexible buried regions; and (3) the slow exchange protons, located in the core region of proteins. Due to technical limit, only the intermediate and slow exchange protons can be practically monitored *semi*-quantitatively within the experimental time frame of this study. A two-exponential decay model (Eq. (2)) was used to describe the exchange reaction of the remaining amide protons. The resolved parameters are summarized in Table 2. F_0, non-exchanged protein fraction at 1-min exposure to D_2O, also reflects the dynamics of the protein. The results of F_0 and Fig. 7 indicated that D138L is more dynamic than that of WT in the absence of cAMP.

4. Discussion

The X-ray crystal structures of *apo*-CAP were recently determined to a resolution of 3.6 Å for *apo*-WT CAP and 2.2 Å for *apo*-D138L CAP, respectively [24]. The structures reveal that DNA recognition helices (F-helices) are buried into the core structure and the two DNA binding domains are dimerized into one rigid body, which explains the low DNA binding affinity in the absence of cAMP. The result of structural comparison of liganded and unliganded WT-CAP suggested that cAMP binding to CAP induces a large conformational change and then stabilizes the active DNA binding conformation through interactions with the C-helices. These changes reorient the subunits and expose the DNA-interacting

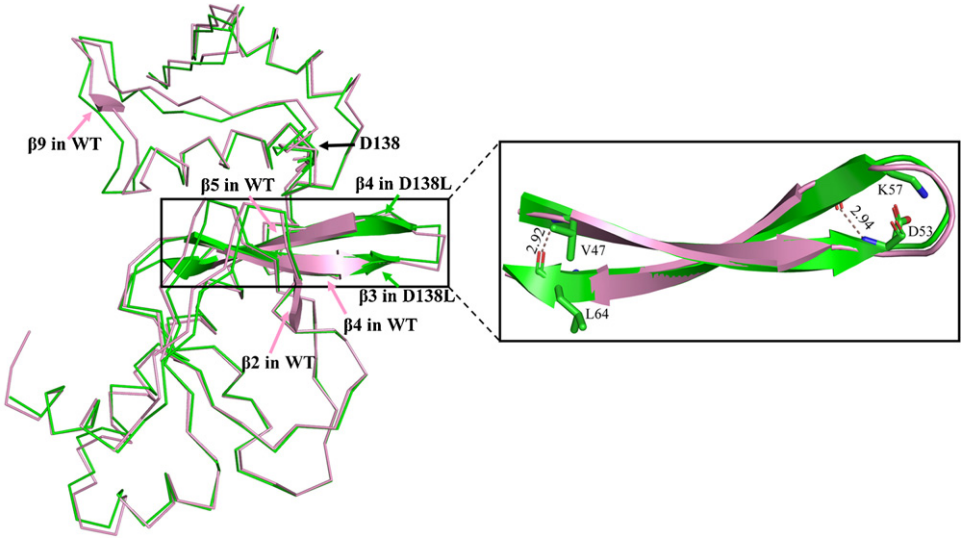

Fig. 4. Comparison of D138L (green) subunit B with WT CAP (pink) closed subunit. For clarity, only the regions that are different are shown in cartoon and the others are shown in ribbon. As a result of lengthened beta sheets (β3 and β4), two more hydrogen bonds are added in D138L which make this area more constrained. (For interpretation of the references to color in this figure legend, the reader is referred to the web version of the article.)

Table 2
Fitted exchange parameters.

CAP	F_0	A_1	A_2	k_1	k_2	c
WT	0.188	0.085 ± 0.001	0.310 ± 0.024	0.192 ± 0.002	0.028 ± 0.01	0.015 ± 0.010
D138L	0.147	0.049 ± 0.004	0.030 ± 0.006	0.130 ± 0.011	0.526 ± 0.072	0.022 ± 0.002

F_0 is non-exchanged fraction at 1-min exposure to D_2O.

helices, which are necessary for CAP to recognize specific DNA sequences [24]. Unfortunately, the resolution of *apo*-WT CAP is insufficient to allow precise explanation of the conformation alteration.

The high resolution structure of D138L CAP–cAMP complex showed that: with the longer C-helix and the shorter D-helix in the liganded D138L, T127 and S128 from opposite helices lie closer to cAMP and both hydrogen bond to the N^6 of the nucleotide. In the liganded D138L, these two residues are at the optimal distance and orientation to interact with cAMP. However, it is not the same in the unliganded D138L because of the shorter C-helix and the longer D-helix. Thus, it is likely that the interaction between N^6 of the adenosine and T127/S128 residues of C-helices stabilizes the liganded conformation.

The closest structure of WT CAP–cAMP complex (PDB code 2GZW) reveals that there are two *syn*-cAMP bound to C-terminal domain, and there is no significant structural difference between D138L CAP–$(cAMP)_4$ and WT CAP–$(cAMP)_4$ (PDB code 2GZW) and both subunits have a "closed" conformation. Furthermore, the reported results of NMR [35,36], molecular dynamics stimulation [37] and small angle neutron scattering [38] have all suggested that WT CAP is symmetric in solution upon binding of cAMP in which the closed form is dominant. Passner and Steitz [5] suggested that the presence of DNA contributed to the third and fourth cAMP binding, however, the structure of our D138L CAP reveals the *syn*-cAMPs can be bound to CAP without DNA, this is consist with the result

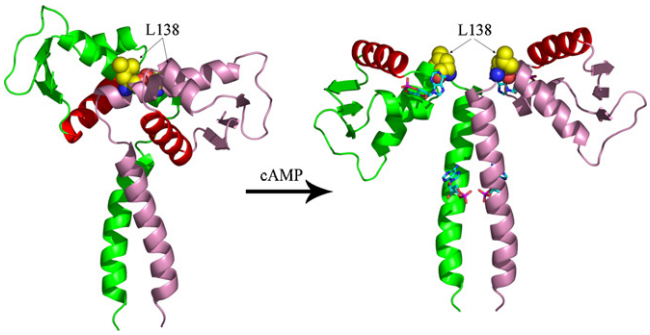

Fig. 5. Unliganded (left) and liganded D138L mutant (right). F-helices are marked in red. The cAMP binding domains have been excluded to emphasize the orientation of the DNA binding domains and the C-helices. Residues L138 were showed in yellow ball. (For interpretation of the references to color in this figure legend, the reader is referred to the web version of the article.)

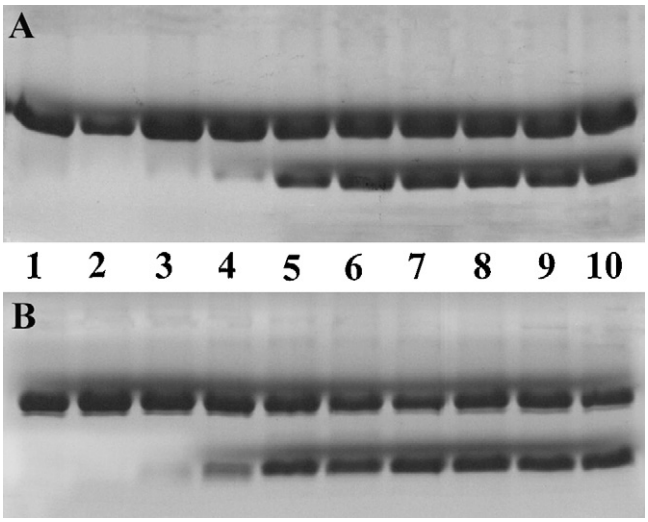

Fig. 6. Proteolytic digestion of CAP by chymotrypsin at various cAMP concentrations. The reaction time was 80 min. Lane 1, CAP alone; lanes 2–10 contained 4 μg/mL protease and concentrations of cAMP: 2, 1 μM; 3, 5 μM; 4, 20 μM; 5, 200 μM; 6, 500 μM; 7, 5 mM; 8, 10 mM; 9, 25 mM; 10, 50 mM. (A): WT CAP. (B): D138L.

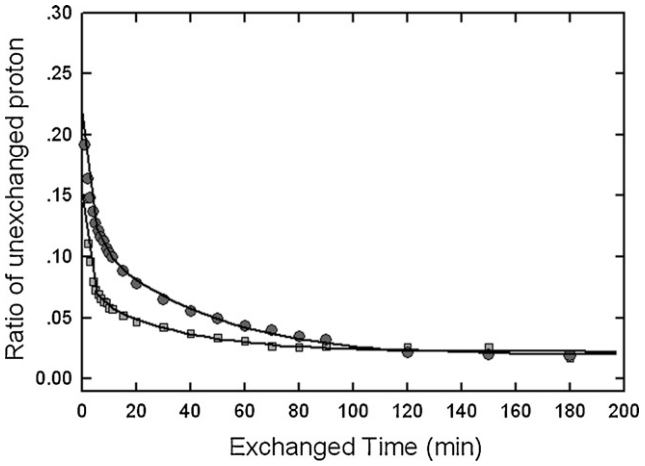

Fig. 7. Global amide proton exchange rates of D138L (solid squares) and WT CAP (solid circles) determined by FT-IR.

of Lee et al. [35]. The biochemical and modeling experiments on certain mutants that bind a maximum of two cAMPs [39] had suggested that the *syn*-cAMP binding sites are additionally formed as a result of the allosteric conformational changes. Thus, the symmetry or asymmetry in crystal structures is probably due to the crystal lattice packing. It is reasonable to speculate that there is no structural change in D138L–cAMP complex between the crystal and the solution structures.

Comparison of the closed subunits of WT CAP–cAMP complex (PDB code 1G6N) and D138L CAP–cAMP complex reveals that the most significant difference appears in the β-flap and loop 3. With new water molecule hydrogen bonded to the amide nitrogen atom of L138 residue, it is reasonable to speculate that the communication network which involves the interfacial interactions between subunits and domains is interrupted, and this interruption blocks the DNA binding domain arriving to its proper orientation that needed for DNA binding under lower cAMP concentration. However, due to the longer β3 and β4 strands, there are two more hydrogen bonds occurring in D138L mutant, resulting in a more constrained conformation. The subtle structural difference may increase the dynamics of D138L mutant, which may facilitate CAP to recognize its cognate DNA sequence.

The K_d of D138L to DNA was lower than that of WT CAP. In the presence of 200 μM cAMP, the binding affinities (K_d) of WT and D138L to *lac* 26 (5′-ATTAATGTGAGTTAGCTCACTCATTA-3′) are 3×10^{-6} M^{-1} and 3.3×10^{-6} M^{-1}, respectively [11]. Recently, protein dynamics have become a focal point in understanding of allosterism [3,11,31]. Subtilisin- and chymotrypsin-generated CAP cores were terminated at residues 134 and 137 respectively, indicating that the results of protease digestion represent the dynamics of the hinge region. In the presence of low cAMP concentration (<200 μM), the digestion of D138L is much faster than that of WT CAP, suggesting that the hinge region of D138L is much more flexible than that of WT in the presence of low cAMP. Meanwhile, FT-IR H–D exchange experiment represents the overall dynamics of CAP. The results clearly indicated that the overall conformation of D138L is much more dynamic than that of WT in the absence of cAMP. These dynamic differences may result in the difference of DNA binding affinity.

In conclusion, the X-ray crystal structure of cAMP-liganded D138L mutant CAP was determined to a resolution of 1.66 Å. This high resolution structure reveals that there are four cAMP binding sites in CAP, both subunits of D138L–cAMP complex are in the "closed" conformation. The interaction between D138 oxygen atom and G141 nitrogen atom is hindered in D138L mutant. A water molecule is hydrogen bonded to the amide nitrogen atom of L138 residue. The loop 3 of the mutant becomes 3 amino acids shorter than that of WT CAP, and the secondary structure alteration provides an additional β sheet hydrogen bond which makes the cAMP binding domain more constrained. These changes make the hinge region more flexible and sensitive to protease. The results of protein dynamic experiments showed that the conformation of D138L mutant is much more dynamic than that of WT, which may impact the recognition of specific DNA sequence.

Acknowledgments

This project was supported in part by the grants from the National Natural Science Foundation of China (30970631 and 30900227), the National Basic Research Program of China (2007CB914304 and 2009CB918600), the Pujiang Program of Shanghai City (No. 09PJD007), and Shanghai Leading Academic Discipline Project (No. B109).

References

[1] J.G. Harman, Biochim. Biophys. Acta 1547 (2001) 1–17.
[2] J.M. Passner, S.C. Schultz, T.A. Steitz, J. Mol. Biol. 304 (2000) 847–859.
[3] H.-S. Won, Y.-S. Lee, S.-H. Lee, B.-J. Lee, Biochim. Biophys. Acta (BBA): Proteins Proteomics 1794 (2009) 1299–1308.
[4] T. Heyduk, J.C. Lee, Proc. Natl. Acad. Sci. U. S. A. 87 (1990) 1744–1748.
[5] J.M. Passner, T.A. Steitz, Proc. Natl. Acad. Sci. U. S. A. 94 (1997) 2843–2847.
[6] S. Ryu, J. Kim, S. Adhya, S. Garges, Proc. Natl. Acad. Sci. U. S. A. 90 (1993) 75–79.
[7] S.C. Schultz, G.C. Shields, T.A. Steitz, Science 253 (1991) 1001–1007.
[8] A.C. Dong, J.M. Malecki, L. Lee, J.F. Carpenter, J.C. Lee, Biochemistry 41 (2002) 6660–6667.
[9] L. Li, V.N. Uversky, A.K. Dunker, S.O. Meroueh, J. Am. Chem. Soc. 129 (2007) 15668–15676.
[10] H. Youn, R.L. Kerby, M. Conrad, G.P. Roberts, J. Biol. Chem. 281 (2006) 1119–1127.
[11] S. Yu, J.C. Lee, Biochemistry 43 (2004) 4662–4669.
[12] I. Kurisaki, K. Fukuzawa, Y. Komeiji, Y. Mochizuki, T. Nakano, J. Imada, A. Chmielewski, S.M. Rothstein, H. Watanabe, S. Tanaka, Biophys. Chem. 130 (2007) 1–9.
[13] K. Omagari, H. Yoshimura, M. Takano, D.Y. Hao, M. Ohmori, A. Sarai, A. Suyama, FEBS Lett. 563 (2004) 55–58.
[14] M.L. DellAcqua, J.D. Scott, J. Biol. Chem. 272 (1997) 12881–12884.
[15] Y. Su, W.R.G. Dostmann, F.W. Herberg, K. Durick, N.H. Xuong, L. Teneyck, S.S. Taylor, K.I. Varughese, Science 269 (1995) 807–813.
[16] J.L. Bos, Nat. Rev. Mol. Cell Biol. 4 (2003) 733–738.
[17] J. de Rooij, F.J.T. Zwartkruis, M.H.G. Verheijen, R.H. Cool, S.M.B. Nijman, A. Wittinghofer, J.L. Bos, Nature 396 (1998) 474–477.
[18] U.B. Kaupp, R. Seifert, Physiol. Rev. 82 (2002) 769–824.
[19] E.C. Young, N. Krougliak, J. Biol. Chem. 279 (2004) 3553–3562.
[20] D.B. McKay, T.A. Steitz, Nature 290 (1981) 744–749.
[21] B. Benoff, H.W. Yang, C.L. Lawson, G. Parkinson, J.S. Liu, E. Blatter, Y.W. Ebright, H.M. Berman, R.H. Ebright, Science 297 (2002) 1562–1566.
[22] D.B. McKay, I.T. Weber, T.A. Steitz, J. Biol. Chem. 257 (1982) 9518–9524.
[23] S.Y. Chu, M. Tordova, G.L. Gilliland, I. Gorshkova, Y. Shi, S.L. Wang, F.P. Schwarz, J. Biol. Chem. 276 (2001) 11230–11236.
[24] H. Sharma, S.N. Yu, J.L. Kong, J.M. Wang, T.A. Steitz, Proc. Natl. Acad. Sci. U. S. A. 106 (2009) 16604–16609.
[25] Z. Otwinowski, W. Minor, Macromol. Crystallogr. PT A (1997) 307–326.
[26] P.D. Adams, R.W. Grosse-Kunstleve, L.W. Hung, T.R. Ioerger, A.J. McCoy, N.W. Moriarty, R.J. Read, J.C. Sacchettini, N.K. Sauter, T.C. Terwilliger, Acta Crystallogr. D: Biol. Crystallogr. 58 (2002) 1948–1954.
[27] P. Emsley, K. Cowtan, Acta Crystallogr. D: Biol. Crystallogr. 60 (2004) 2126–2132.
[28] S. Bailey, Acta Crystallogr. D: Biol. Crystallogr. 50 (1994) 760–763.
[29] S.N. Yu, F.H. Fan, S.C. Flores, F. Mei, X.D. Cheng, Biochemistry 45 (2006) 15318–15326.
[30] S.N. Yu, L.L.Y. Lee, J.C. Lee, Biophys. Chem. 103 (2003) 1–11.
[31] S.H. Lin, L. Kovac, A.J. Chin, C.C. Chin, J.C. Lee, Biochemistry 41 (2002) 2946–2955.
[32] E. Heyduk, T. Heyduk, J.C. Lee, Biochemistry 31 (1992) 3682–3688.
[33] H.H.J. de Jongh, E. Goormaghtigh, J.M. Ruysschaert, Biochemistry 36 (1997) 13593–13602.
[34] J.Q. Li, X.D. Cheng, J.C. Lee, Biochemistry 41 (2002) 14771–14778.
[35] T.W. Lee, H.S. Won, S.H. Park, Y. Kyogoku, B.J. Lee, J. Biochem. 130 (2001) 57–61.
[36] H.S. Won, T.W. Lee, S.H. Park, B.J. Lee, J. Biol. Chem. 277 (2002) 11450–11455.
[37] M. Berrera, S. Pantano, P. Carloni, J. Phys. Chem. B 111 (2007) 1496–1501.
[38] S. Krueger, I. Gorshkova, J. Brown, J. Hoskins, K.H. McKenney, F.P. Schwarz, J. Biol. Chem. 273 (1998) 20001–20006.
[39] S.P. Scott, S. Jarjous, Biochemistry 44 (2005) 8730–8748.